Measurement of the Decay $\Xi^0 \to \Lambda\gamma$ with Entangled $\Xi^0\bar{\Xi}^0$ Pairs

M. Ablikim[1], M. N. Achasov[4,c], P. Adlarson[76], O. Afedulidis[3], X. C. Ai[81], R. Aliberti[35], A. Amoroso[75A,75C], Q. An[72,58,a], Y. Bai[57], O. Bakina[36], I. Balossino[29A], Y. Ban[46,h], H.-R. Bao[64], V. Batozskaya[1,44], K. Begzsuren[32], N. Berger[35], M. Berlowski[44], M. Bertani[28A], D. Bettoni[29A], F. Bianchi[75A,75C], E. Bianco[75A,75C], A. Bortone[75A,75C], I. Boyko[36], R. A. Briere[5], A. Brueggemann[69], H. Cai[77], X. Cai[1,58], A. Calcaterra[28A], G. F. Cao[1,64], N. Cao[1,64], S. A. Cetin[62A], J. F. Chang[1,58], G. R. Che[43], G. Chelkov[36,b], C. Chen[43], C. H. Chen[9], Chao Chen[55], G. Chen[1], H. S. Chen[1,64], H. Y. Chen[20], M. L. Chen[1,58,64], S. J. Chen[42], S. L. Chen[45], S. M. Chen[61], T. Chen[1,64], X. R. Chen[31,64], X. T. Chen[1,64], Y. B. Chen[1,58], Y. Q. Chen[34], Z. J. Chen[25,i], Z. Y. Chen[1,64], S. K. Choi[10A], G. Cibinetto[29A], F. Cossio[75C], J. J. Cui[50], H. L. Dai[1,58], J. P. Dai[79], A. Dbeyssi[18], R. E. de Boer[3], D. Dedovich[36], C. Q. Deng[73], Z. Y. Deng[1], A. Denig[35], I. Denysenko[36], M. Destefanis[75A,75C], F. De Mori[75A,75C], B. Ding[67,1], X. X. Ding[46,h], Y. Ding[40], Y. Ding[34], J. Dong[1,58], L. Y. Dong[1,64], M. Y. Dong[1,58,64], X. Dong[77], M. C. Du[1], S. X. Du[81], Y. Y. Duan[55], Z. H. Duan[42], P. Egorov[36,b], Y. H. Fan[45], J. Fang[1,58], J. Fang[59], S. S. Fang[1,64], W. X. Fang[1], Y. Fang[1], Y. Q. Fang[1,58], R. Farinelli[29A], L. Fava[75B,75C], F. Feldbauer[3], G. Felici[28A], C. Q. Feng[72,58], J. H. Feng[59], Y. T. Feng[72,58], M. Fritsch[3], C. D. Fu[1], J. L. Fu[64], Y. W. Fu[1,64], H. Gao[64], X. B. Gao[41], Y. N. Gao[46,h], Yang Gao[72,58], S. Garbolino[75C], I. Garzia[29A,29B], L. Ge[81], P. T. Ge[19], Z. W. Ge[42], C. Geng[59], E. M. Gersabeck[68], A. Gilman[70], K. Goetzen[13], L. Gong[40], W. X. Gong[1,58], W. Gradl[35], S. Gramigna[29A,29B], M. Greco[75A,75C], M. H. Gu[1,58], Y. T. Gu[15], C. Y. Guan[1,64], A. Q. Guo[31,64], L. B. Guo[41], M. J. Guo[50], R. P. Guo[49], Y. P. Guo[12,g], A. Guskov[36,b], J. Gutierrez[27], K. L. Han[64], T. T. Han[1], F. Hanisch[3], X. Q. Hao[19], F. A. Harris[66], K. K. He[55], K. L. He[1,64], F. H. Heinsius[3], C. H. Heinz[35], Y. K. Heng[1,58,64], C. Herold[60], T. Holtmann[3], P. C. Hong[34], G. Y. Hou[1,64], X. T. Hou[1,64], Y. R. Hou[64], Z. L. Hou[1], B. Y. Hu[59], H. M. Hu[1,64], J. F. Hu[56,j], S. L. Hu[12,g], T. Hu[1,58,64], Y. Hu[1], G. S. Huang[72,58], K. X. Huang[59], L. Q. Huang[31,64], X. T. Huang[50], Y. P. Huang[1], Y. S. Huang[59], T. Hussain[74], F. Hölzken[3], N. Hüsken[35], N. in der Wiesche[69], J. Jackson[27], S. Janchiv[32], J. H. Jeong[10A], Q. Ji[1], Q. P. Ji[19], W. Ji[1,64], X. B. Ji[1,64], X. L. Ji[1,58], Y. Y. Ji[50], X. Q. Jia[50], Z. K. Jia[72,58], D. Jiang[1,64], H. B. Jiang[77], P. C. Jiang[46,h], S. S. Jiang[39], T. J. Jiang[16], X. S. Jiang[1,58,64], Y. Jiang[64], J. B. Jiao[50], J. K. Jiao[34], Z. Jiao[23], S. Jin[42], Y. Jin[67], M. Q. Jing[1,64], X. M. Jing[64], T. Johansson[76], S. Kabana[33], N. Kalantar-Nayestanaki[65], X. L. Kang[9], X. S. Kang[40], M. Kavatsyuk[65], B. C. Ke[81], V. Khachatryan[27], A. Khoukaz[69], R. Kiuchi[1], O. B. Kolcu[62A], B. Kopf[3], M. Kuessner[3], X. Kui[1,64], N. Kumar[26], A. Kupsc[44,76], W. Kühn[37], J. J. Lane[68], L. Lavezzi[75A,75C], T. T. Lei[72,58], Z. H. Lei[72,58], M. Lellmann[35], T. Lenz[35], C. Li[47], C. Li[43], C. H. Li[39], Cheng Li[72,58], D. M. Li[81], F. Li[1,58], G. Li[1], H. B. Li[1,64], H. J. Li[19], H. N. Li[56,j], Hui Li[43], J. R. Li[61], J. S. Li[59], K. Li[1], L. J. Li[1,64], L. K. Li[1], Lei Li[48], M. H. Li[43], P. R. Li[38,k,l], Q. M. Li[1,64], Q. X. Li[50], R. Li[17,31], S. X. Li[12], T. Li[50], W. D. Li[1,64], W. G. Li[1,a], X. Li[1,64], X. H. Li[72,58], X. L. Li[50], X. Y. Li[1,64], X. Z. Li[59], Y. G. Li[46,h], Z. J. Li[59], Z. Y. Li[79], C. Liang[42], H. Liang[72,58], H. Liang[1,64], Y. F. Liang[54], Y. T. Liang[31,64], G. R. Liao[14], Y. P. Liao[1,64], J. Libby[26], A. Limphirat[60], C. C. Lin[55], D. X. Lin[31,64], T. Lin[1], B. J. Liu[1], B. X. Liu[77], C. Liu[34], C. X. Liu[1], F. Liu[1], F. H. Liu[53], Feng Liu[6], G. M. Liu[56,j], H. Liu[38,k,l], H. B. Liu[15], H. H. Liu[1], H. M. Liu[1,64], Huihui Liu[21], J. B. Liu[72,58], J. Y. Liu[1,64], K. Liu[38,k,l], K. Y. Liu[40], Ke Liu[22], L. Liu[72,58], L. C. Liu[43], Lu Liu[43], M. H. Liu[12,g], P. L. Liu[1], Q. Liu[64], S. B. Liu[72,58], T. Liu[12,g], W. K. Liu[43], W. M. Liu[72,58], X. Liu[39], X. Liu[38,k,l], Y. Liu[81], Y. Liu[38,k,l], Y. B. Liu[43], Z. A. Liu[1,58,64], Z. D. Liu[9], Z. Q. Liu[50], X. C. Lou[1,58,64], F. X. Lu[59], H. J. Lu[23], J. G. Lu[1,58], X. L. Lu[1], Y. Lu[7], Y. P. Lu[1,58], Z. H. Lu[1,64], C. L. Luo[41], J. R. Luo[59], M. X. Luo[80], T. Luo[12,g], X. L. Luo[1,58], X. R. Lyu[64], Y. F. Lyu[43], F. C. Ma[40], H. Ma[79], H. L. Ma[1], J. L. Ma[1,64], L. L. Ma[50], L. R. Ma[67], M. M. Ma[1,64], Q. M. Ma[1], R. Q. Ma[1,64], T. Ma[72,58], X. T. Ma[1,64], X. Y. Ma[1,58], Y. Ma[46,h], Y. M. Ma[31], F. E. Maas[18], M. Maggiora[75A,75C], S. Malde[70], Y. J. Mao[46,h], Z. P. Mao[1], S. Marcello[75A,75C], Z. X. Meng[67], J. G. Messchendorp[13,65], G. Mezzadri[29A], H. Miao[1,64], T. J. Min[42], R. E. Mitchell[27], X. H. Mo[1,58,64], B. Moses[27], N. Yu. Muchnoi[4,c], J. Muskalla[35], Y. Nefedov[36], F. Nerling[18,e], L. S. Nie[20], I. B. Nikolaev[4,c], Z. Ning[1,58], S. Nisar[11,m], Q. L. Niu[38,k,l], W. D. Niu[55], Y. Niu[50], S. L. Olsen[64], Q. Ouyang[1,58,64], S. Pacetti[28B,28C], X. Pan[55], Y. Pan[57], A. Pathak[34], Y. P. Pei[72,58], M. Pelizaeus[3], H. P. Peng[72,58], Y. Y. Peng[38,k,l], K. Peters[13,e], J. L. Ping[41], R. G. Ping[1,64], S. Plura[35], V. Prasad[33], F. Z. Qi[1], H. Qi[72,58], H. R. Qi[61], M. Qi[42], T. Y. Qi[12,g], S. Qian[1,58], W. B. Qian[64], C. F. Qiao[64], X. K. Qiao[81], J. J. Qin[73], L. Q. Qin[14], L. Y. Qin[72,58], X. P. Qin[12,g], X. S. Qin[50], Z. H. Qin[1,58], J. F. Qiu[1], Z. H. Qu[73], C. F. Redmer[35], K. J. Ren[39], A. Rivetti[75C], M. Rolo[75C], G. Rong[1,64], Ch. Rosner[18], S. N. Ruan[43], N. Salone[44], A. Sarantsev[36,d], Y. Schelhaas[35], K. Schoenning[76], M. Scodeggio[29A], K. Y. Shan[12,g], W. Shan[24], X. Y. Shan[72,58], Z. J. Shang[38,k,l], J. F. Shangguan[16], L. G. Shao[1,64], M. Shao[72,58], C. P. Shen[12,g], H. F. Shen[1,8], W. H. Shen[64], X. Y. Shen[1,64], B. A. Shi[64], H. Shi[72,58], H. C. Shi[72,58],

J. L. Shi[12,g], J. Y. Shi[1], Q. Q. Shi[55], S. Y. Shi[73], X. Shi[1,58], J. J. Song[19], T. Z. Song[59], W. M. Song[34,1], Y. J. Song[12,g], Y. X. Song[46,h,n], S. Sosio[75A,75C], S. Spataro[75A,75C], F. Stieler[35], Y. J. Su[64], G. B. Sun[77], G. X. Sun[1], H. Sun[64], H. K. Sun[1], J. F. Sun[19], K. Sun[61], L. Sun[77], S. S. Sun[1,64], T. Sun[51,f], W. Y. Sun[34], Y. Sun[9], Y. J. Sun[72,58], Y. Z. Sun[1], Z. Q. Sun[1,64], Z. T. Sun[50], C. J. Tang[54], G. Y. Tang[1], J. Tang[59], M. Tang[72,58], Y. A. Tang[77], L. Y. Tao[73], Q. T. Tao[25,i], M. Tat[70], J. X. Teng[72,58], V. Thoren[76], W. H. Tian[59], Y. Tian[31,64], Z. F. Tian[77], I. Uman[62B], Y. Wan[55], S. J. Wang [50], B. Wang[1], B. L. Wang[64], Bo Wang[72,58], D. Y. Wang[46,h], F. Wang[73], H. J. Wang[38,k,l], J. J. Wang[77], J. P. Wang [50], K. Wang[1,58], L. L. Wang[1], M. Wang[50], N. Y. Wang[64], S. Wang[12,g], S. Wang[38,k,l], T. Wang[12,g], T. J. Wang[43], W. Wang[73], W. Wang[59], W. P. Wang[35,72,o], W. P. Wang[72,58], X. Wang[46,h], X. F. Wang[38,k,l], X. J. Wang[39], X. L. Wang[12,g], X. N. Wang[1], Y. Wang[61], Y. D. Wang[45], Y. F. Wang[1,58,64], Y. L. Wang[19], Y. N. Wang[45], Y. Q. Wang[1], Yaqian Wang[17], Yi Wang[61], Z. Wang[1,58], Z. L. Wang[73], Z. Y. Wang[1,64], Ziyi Wang[64], D. H. Wei[14], F. Weidner[69], S. P. Wen[1], Y. R. Wen[39], U. Wiedner[3], G. Wilkinson[70], M. Wolke[76], L. Wollenberg[3], C. Wu[39], J. F. Wu[1,8], L. H. Wu[1], L. J. Wu[1,64], X. Wu[12,g], X. H. Wu[34], Y. Wu[72,58], Y. H. Wu[55], Y. J. Wu[31], Z. Wu[1,58], L. Xia[72,58], X. M. Xian[39], B. H. Xiang[1,64], T. Xiang[46,h], D. Xiao[38,k,l], G. Y. Xiao[42], S. Y. Xiao[1], Y. L. Xiao[12,g], Z. J. Xiao[41], C. Xie[42], X. H. Xie[46,h], Y. Xie[50], Y. G. Xie[1,58], Y. H. Xie[6], Z. P. Xie[72,58], T. Y. Xing[1,64], C. F. Xu[1,64], C. J. Xu[59], G. F. Xu[1], H. Y. Xu[67,2,p], M. Xu[72,58], Q. J. Xu[16], Q. N. Xu[30], W. Xu[1], W. L. Xu[67], X. P. Xu[55], Y. C. Xu[78], Z. S. Xu[64], F. Yan[12,g], L. Yan[12,g], W. B. Yan[72,58], W. C. Yan[81], X. Q. Yan[1,64], H. J. Yang[51,f], H. L. Yang[34], H. X. Yang[1], T. Yang[1], Y. Yang[12,g], Y. F. Yang[1,64], Y. F. Yang[43], Y. X. Yang[1,64], Z. W. Yang[38,k,l], Z. P. Yao[50], M. Ye[1,58], M. H. Ye[8], J. H. Yin[1], Junhao Yin[43], Z. Y. You[59], B. X. Yu[1,58,64], C. X. Yu[43], G. Yu[1,64], J. S. Yu[25,i], T. Yu[73], X. D. Yu[46,h], Y. C. Yu[81], C. Z. Yuan[1,64], J. Yuan[45], J. Yuan[34], L. Yuan[2], S. C. Yuan[1,64], Y. Yuan[1,64], Z. Y. Yuan[59], C. X. Yue[39], A. A. Zafar[74], F. R. Zeng[50], S. H. Zeng[63A,63B,63C,63D], X. Zeng[12,g], Y. Zeng[25,i], Y. J. Zeng[59], Y. J. Zeng[1,64], X. Y. Zhai[34], Y. C. Zhai[50], Y. H. Zhan[59], A. Q. Zhang[1,64], B. L. Zhang[1,64], B. X. Zhang[1], D. H. Zhang[43], G. Y. Zhang[19], H. Zhang[81], H. Zhang[72,58], H. C. Zhang[1,58,64], H. H. Zhang[59], H. H. Zhang[34], H. Q. Zhang[1,58,64], H. R. Zhang[72,58], H. Y. Zhang[1,58], J. Zhang[81], J. Zhang[59], J. J. Zhang[52], J. L. Zhang[20], J. Q. Zhang[41], J. S. Zhang[12,g], J. W. Zhang[1,58,64], J. X. Zhang[38,k,l], J. Y. Zhang[1], J. Z. Zhang[1,64], Jianyu Zhang[64], L. M. Zhang[61], Lei Zhang[42], P. Zhang[1,64], Q. Y. Zhang[34], R. Y. Zhang[38,k,l], S. H. Zhang[1,64], Shulei Zhang[25,i], X. D. Zhang[45], X. M. Zhang[1], X. Y. Zhang[50], Y. Zhang[73], Y. Zhang[1], Y. T. Zhang[81], Y. H. Zhang[1,58], Y. M. Zhang[39], Yan Zhang[72,58], Z. D. Zhang[1], Z. H. Zhang[1], Z. L. Zhang[34], Z. Y. Zhang[43], Z. Y. Zhang[77], Z. Z. Zhang[45], G. Zhao[1], J. Y. Zhao[1,64], J. Z. Zhao[1,58], L. Zhao[1], Lei Zhao[72,58], M. G. Zhao[43], N. Zhao[79], R. P. Zhao[64], S. J. Zhao[81], Y. B. Zhao[1,58], Y. X. Zhao[31,64], Z. G. Zhao[72,58], A. Zhemchugov[36,b], B. Zheng[73], B. M. Zheng[34], J. P. Zheng[1,58], W. J. Zheng[1,64], Y. H. Zheng[64], B. Zhong[41], X. Zhong[59], H. Zhou[50], J. Y. Zhou[34], L. P. Zhou[1,64], S. Zhou[6], X. Zhou[77], X. K. Zhou[6], X. R. Zhou[72,58], X. Y. Zhou[39], Y. Z. Zhou[12,g], A. N. Zhu[64], J. Zhu[43], K. Zhu[1], K. J. Zhu[1,58,64], K. S. Zhu[12,g], L. Zhu[34], L. X. Zhu[64], S. H. Zhu[71], T. J. Zhu[12,g], W. D. Zhu[41], Y. C. Zhu[72,58], Z. A. Zhu[1,64], J. H. Zou[1], J. Zu[72,58]

(BESIII Collaboration)

[1] *Institute of High Energy Physics, Beijing 100049, People's Republic of China*
[2] *Beihang University, Beijing 100191, People's Republic of China*
[3] *Bochum Ruhr-University, D-44780 Bochum, Germany*
[4] *Budker Institute of Nuclear Physics SB RAS (BINP), Novosibirsk 630090, Russia*
[5] *Carnegie Mellon University, Pittsburgh, Pennsylvania 15213, USA*
[6] *Central China Normal University, Wuhan 430079, People's Republic of China*
[7] *Central South University, Changsha 410083, People's Republic of China*
[8] *China Center of Advanced Science and Technology, Beijing 100190, People's Republic of China*
[9] *China University of Geosciences, Wuhan 430074, People's Republic of China*
[10] *Chung-Ang University, Seoul, 06974, Republic of Korea*
[11] *COMSATS University Islamabad, Lahore Campus, Defence Road, Off Raiwind Road, 54000 Lahore, Pakistan*
[12] *Fudan University, Shanghai 200433, People's Republic of China*
[13] *GSI Helmholtzcentre for Heavy Ion Research GmbH, D-64291 Darmstadt, Germany*
[14] *Guangxi Normal University, Guilin 541004, People's Republic of China*
[15] *Guangxi University, Nanning 530004, People's Republic of China*
[16] *Hangzhou Normal University, Hangzhou 310036, People's Republic of China*

[17] *Hebei University, Baoding 071002, People's Republic of China*

[18] *Helmholtz Institute Mainz, Staudinger Weg 18, D-55099 Mainz, Germany*

[19] *Henan Normal University, Xinxiang 453007, People's Republic of China*

[20] *Henan University, Kaifeng 475004, People's Republic of China*

[21] *Henan University of Science and Technology, Luoyang 471003, People's Republic of China*

[22] *Henan University of Technology, Zhengzhou 450001, People's Republic of China*

[23] *Huangshan College, Huangshan 245000, People's Republic of China*

[24] *Hunan Normal University, Changsha 410081, People's Republic of China*

[25] *Hunan University, Changsha 410082, People's Republic of China*

[26] *Indian Institute of Technology Madras, Chennai 600036, India*

[27] *Indiana University, Bloomington, Indiana 47405, USA*

[28] *INFN Laboratori Nazionali di Frascati , (A)INFN Laboratori Nazionali di Frascati, I-00044, Frascati, Italy; (B)INFN Sezione di Perugia, I-06100, Perugia, Italy; (C)University of Perugia, I-06100, Perugia, Italy*

[29] *INFN Sezione di Ferrara, (A)INFN Sezione di Ferrara, I-44122, Ferrara, Italy; (B)University of Ferrara, I-44122, Ferrara, Italy*

[30] *Inner Mongolia University, Hohhot 010021, People's Republic of China*

[31] *Institute of Modern Physics, Lanzhou 730000, People's Republic of China*

[32] *Institute of Physics and Technology, Peace Avenue 54B, Ulaanbaatar 13330, Mongolia*

[33] *Instituto de Alta Investigación, Universidad de Tarapacá, Casilla 7D, Arica 1000000, Chile*

[34] *Jilin University, Changchun 130012, People's Republic of China*

[35] *Johannes Gutenberg University of Mainz, Johann-Joachim-Becher-Weg 45, D-55099 Mainz, Germany*

[36] *Joint Institute for Nuclear Research, 141980 Dubna, Moscow region, Russia*

[37] *Justus-Liebig-Universitaet Giessen, II. Physikalisches Institut, Heinrich-Buff-Ring 16, D-35392 Giessen, Germany*

[38] *Lanzhou University, Lanzhou 730000, People's Republic of China*

[39] *Liaoning Normal University, Dalian 116029, People's Republic of China*

[40] *Liaoning University, Shenyang 110036, People's Republic of China*

[41] *Nanjing Normal University, Nanjing 210023, People's Republic of China*

[42] *Nanjing University, Nanjing 210093, People's Republic of China*

[43] *Nankai University, Tianjin 300071, People's Republic of China*

[44] *National Centre for Nuclear Research, Warsaw 02-093, Poland*

[45] *North China Electric Power University, Beijing 102206, People's Republic of China*

[46] *Peking University, Beijing 100871, People's Republic of China*

[47] *Qufu Normal University, Qufu 273165, People's Republic of China*

[48] *Renmin University of China, Beijing 100872, People's Republic of China*

[49] *Shandong Normal University, Jinan 250014, People's Republic of China*

[50] *Shandong University, Jinan 250100, People's Republic of China*

[51] *Shanghai Jiao Tong University, Shanghai 200240, People's Republic of China*

[52] *Shanxi Normal University, Linfen 041004, People's Republic of China*

[53] *Shanxi University, Taiyuan 030006, People's Republic of China*

[54] *Sichuan University, Chengdu 610064, People's Republic of China*

[55] *Soochow University, Suzhou 215006, People's Republic of China*

[56] *South China Normal University, Guangzhou 510006, People's Republic of China*

[57] *Southeast University, Nanjing 211100, People's Republic of China*

[58] *State Key Laboratory of Particle Detection and Electronics, Beijing 100049, Hefei 230026, People's Republic of China*

[59] *Sun Yat-Sen University, Guangzhou 510275, People's Republic of China*

[60] *Suranaree University of Technology, University Avenue 111, Nakhon Ratchasima 30000, Thailand*

[61] *Tsinghua University, Beijing 100084, People's Republic of China*

[62] *Turkish Accelerator Center Particle Factory Group, (A)Istinye University, 34010, Istanbul, Turkey; (B)Near East University, Nicosia, North Cyprus, 99138, Mersin 10, Turkey*

[63] *University of Bristol, (A)H H Wills Physics Laboratory; (B)Tyndall Avenue; (C)Bristol; (D)BS8 1TL*

[64] *University of Chinese Academy of Sciences, Beijing 100049, People's Republic of China*
[65] *University of Groningen, NL-9747 AA Groningen, The Netherlands*
[66] *University of Hawaii, Honolulu, Hawaii 96822, USA*
[67] *University of Jinan, Jinan 250022, People's Republic of China*
[68] *University of Manchester, Oxford Road, Manchester, M13 9PL, United Kingdom*
[69] *University of Muenster, Wilhelm-Klemm-Strasse 9, 48149 Muenster, Germany*
[70] *University of Oxford, Keble Road, Oxford OX13RH, United Kingdom*
[71] *University of Science and Technology Liaoning, Anshan 114051, People's Republic of China*
[72] *University of Science and Technology of China, Hefei 230026, People's Republic of China*
[73] *University of South China, Hengyang 421001, People's Republic of China*
[74] *University of the Punjab, Lahore-54590, Pakistan*
[75] *University of Turin and INFN, (A)University of Turin, I-10125, Turin, Italy; (B)University of Eastern Piedmont, I-15121, Alessandria, Italy; (C)INFN, I-10125, Turin, Italy*
[76] *Uppsala University, Box 516, SE-75120 Uppsala, Sweden*
[77] *Wuhan University, Wuhan 430072, People's Republic of China*
[78] *Yantai University, Yantai 264005, People's Republic of China*
[79] *Yunnan University, Kunming 650500, People's Republic of China*
[80] *Zhejiang University, Hangzhou 310027, People's Republic of China*
[81] *Zhengzhou University, Zhengzhou 450001, People's Republic of China*

[a] *Deceased*
[b] *Also at the Moscow Institute of Physics and Technology, Moscow 141700, Russia*
[c] *Also at the Novosibirsk State University, Novosibirsk, 630090, Russia*
[d] *Also at the NRC "Kurchatov Institute", PNPI, 188300, Gatchina, Russia*
[e] *Also at Goethe University Frankfurt, 60323 Frankfurt am Main, Germany*
[f] *Also at Key Laboratory for Particle Physics, Astrophysics and Cosmology, Ministry of Education; Shanghai Key Laboratory for Particle Physics and Cosmology; Institute of Nuclear and Particle Physics, Shanghai 200240, People's Republic of China*
[g] *Also at Key Laboratory of Nuclear Physics and Ion-beam Application (MOE) and Institute of Modern Physics, Fudan University, Shanghai 200443, People's Republic of China*
[h] *Also at State Key Laboratory of Nuclear Physics and Technology, Peking University, Beijing 100871, People's Republic of China*
[i] *Also at School of Physics and Electronics, Hunan University, Changsha 410082, China*
[j] *Also at Guangdong Provincial Key Laboratory of Nuclear Science, Institute of Quantum Matter, South China Normal University, Guangzhou 510006, China*
[k] *Also at MOE Frontiers Science Center for Rare Isotopes, Lanzhou University, Lanzhou 730000, People's Republic of China*
[l] *Also at Lanzhou Center for Theoretical Physics, Lanzhou University, Lanzhou 730000, People's Republic of China*
[m] *Also at the Department of Mathematical Sciences, IBA, Karachi 75270, Pakistan*
[n] *Also at Ecole Polytechnique Federale de Lausanne (EPFL), CH-1015 Lausanne, Switzerland*
[o] *Also at Helmholtz Institute Mainz, Staudinger Weg 18, D-55099 Mainz, Germany*
[p] *Also at School of Physics, Beihang University, Beijing 100191 , China*
(Dated: September 2, 2024)

In this Letter, a systematic study of the weak radiative hyperon decay $\Xi^0 \to \Lambda\gamma$ at an electron-positron collider using entangled $\Xi^0\bar{\Xi}^0$ pair events is presented. The absolute branching fraction for this decay has been measured for the first time, and is $(1.347 \pm 0.066_{\text{stat.}} \pm 0.054_{\text{syst.}}) \times 10^{-3}$. The decay asymmetry parameter, which characterizes the effect of parity violation in the decay, is determined to be $-0.741 \pm 0.062_{\text{stat.}} \pm 0.019_{\text{syst.}}$. The obtained results are consistent with the world average values within the uncertainties, offering valuable insights into the underlying mechanism governing the weak radiative hyperon decays. The charge conjugation parity (CP) symmetries of branching fraction and decay asymmetry parameter in the decay are also studied. No statistically significant violation of charge conjugation parity symmetry is observed.

The ground-state hyperons have played a crucial role in the understanding of weak interactions. However,

numerous unanswered questions persist regarding the weak decay mechanisms and the role of hyperons in non-perturbative quantum chromodynamics (QCD) [1, 2]. Specifically, weak radiative hyperon decays (WRHDs) provide valuable insights into the nature of nonleptonic weak interactions [3]. In general, the radiative decays of a spin-$\frac{1}{2}$ hyperon consist of a parity conserving (P-wave) and a parity violating (S-wave) amplitude. The decay asymmetry parameter α_γ, determined by the phase difference between S- and P-waves, can be measured from the asymmetric decay angle distribution of the final state baryon and presents a longstanding puzzle in WRHDs [4]. Although decay asymmetries of $\Sigma^+ \to p\gamma$ and $\Xi^- \to \Sigma^-\gamma$ decays are expected to be zero under SU(3) symmetry, experiments have measured non-zero values for these [5, 6]. Various phenomenological models have been proposed to explain the experimental results [7–11], however, none of them provide a unified description of all WRHDs. In particular, the insufficiency of short-distance contributions (e.g. W-exchange processes [12]) to the large decay asymmetries indicates a substantial contribution from non-perturbative QCD effects. To make further progress towards solving this puzzle, new and more precise measurements of any WRHD are desired [13, 14].

It is widely believed in the scientific community that the violation of the combined charge conjugation and parity symmetries (CP) is essential for elucidating the matter-antimatter asymmetry in the universe [15]. The current observed CP asymmetries [16] and the predictions of the standard model (SM) through the introduction of a single weak phase in the Cabibbo-Kobayashi-Maskawa matrix [2] are insufficient in explaining the observed matter-antimatter asymmetry. This has led to a surge in studies of CP violation beyond weak hadronic decays and beyond the SM. Weak radiative decays of s quark [17], c quark [18] and b quark [19] are sensitive to new physics beyond the SM [20] and may exhibit over 10 % CP asymmetry in some models [19, 21]. The situation is less clear for baryons compared to mesons due to the complexity of their systems [22]. Experimentally, though weak radiative decays of heavy mesons have been studied thoroughly [23], measurements in the baryon sector are very limited [24, 25]. Due to complex non-perturbative QCD effects, CP asymmetries in WRHDs, which involve an s quark, are more complicated for theory predictions than in Λ_c, Λ_b, and other heavy baryons. Nevertheless, they are experimentally attractive because of the larger branching fractions (BFs) at the level of $\mathcal{O}(10^{-3})$.

The decay $\Xi^0 \to \Lambda\gamma$ is a fundamental process for the study of WRHDs. The current experimental results on hyperon nonleptonic decays and magnetic moments provide a reliable prediction on the P-wave amplitude of $\Xi^0 \to \Lambda\gamma$ [26]. Therefore, its α_γ serves as a crucial value to confirm the sources of the S-wave amplitude in

WRHDs. On the other hand, a chiral perturbation theory (ChPT) for baryons can be constructed with only a few input parameters [13]. In baryon ChPT, a low energy constant C_ρ describes the direct photon emission contribution to the real part of the S-wave amplitude at tree level. To date, C_ρ can only be determined through the processes $\Xi^0 \to \Lambda\gamma$ and $\Xi^0 \to \Sigma^0\gamma$. Therefore, robust and precise experimental results are urgently needed for improving the theory. Although studies of $\Xi^0 \to \Lambda\gamma$ have been performed with ever-increasing statistics at fixed target experiments [6, 27–29], all the measured BFs have been reported as relative values to the BF of $\Xi^0 \to \Lambda\pi^0$. Furthermore, the systematic uncertainty is dominating the precision of BF and α_γ measurements.

The observation of hyperon transverse polarization in the decays $J/\psi \to B\bar{B}$ ($B = \Lambda, \Sigma^{\pm,0}, \Xi^{-,0}$) at BESIII has opened a new territory to study the character of hyperon decays [30–32]. The unique spin entanglement information present in hyperon pairs enhances the statistical sensitivity to α_γ compared to fixed target experiments [29] by several times with the same sample sizes [33]. Additionally, the application of the double-tag (DT) method [34] enables the measurement of absolute BFs with lower systematic uncertainty. These advantages have been validated in the studies of the decays $\Lambda \to n\gamma$ [35] and $\Sigma^+ \to p\gamma$ [25] at BESIII, where significant deviations of BFs from the world average values [36] have been observed.

In this Letter, using the $J/\psi \to \Xi^0(\to \Lambda\gamma)\bar{\Xi}^0(\to \bar{\Lambda}\pi^0)$ decay based on $(10\,087 \pm 44) \times 10^6$ J/ψ events [37] collected at BESIII, we report measurements of the absolute BF and the decay asymmetry parameter of $\Xi^0 \to \Lambda\gamma$, as well as a potential CP asymmetry in the decay. Throughout this Letter, charge conjugation (c.c.) is always implied and Λ is reconstructed using its decay $\Lambda \to p\pi^-$, unless explicitly noted otherwise.

A detailed description of the design and performance of the BESIII detector can be found in Ref. [38], while the simulation and analysis software framework for BESIII is described in Refs. [39]. A double-tag method [34] is employed for event selection. To search for the decay $\Xi^0 \to \Lambda\gamma$, events of $J/\psi \to \Xi^0\bar{\Xi}^0$ are tagged by reconstructing a $\bar{\Xi}^0$ signal (named 'single-tag (ST)' events) using its dominant decay channel $\bar{\Xi}^0 \to \bar{\Lambda}\pi^0$. Subsequently, the signal $\Xi^0 \to \Lambda\gamma$ is searched for in the system recoiling against the ST $\bar{\Xi}^0$ (named 'DT'). The absolute BF is calculated by $\mathrm{BF}(\Xi^0 \to \Lambda\gamma) = \frac{N_{\mathrm{DT}}^{\mathrm{obs}}}{N_{\mathrm{ST}}^{\mathrm{obs}}} \frac{\varepsilon_{\mathrm{ST}}}{\varepsilon_{\mathrm{DT}}} \frac{1}{\mathrm{BF}_{\Lambda \to p\pi^-}}$, where $N_{\mathrm{ST(DT)}}^{\mathrm{obs}}$ and $\varepsilon_{\mathrm{ST(DT)}}$ are the ST (DT) yields and the corresponding detection efficiencies, and $\mathrm{BF}_{\Lambda \to p\pi^-}$ is the BF of $\Lambda \to p\pi^-$.

A general formula for the differential cross sections of the signal $J/\psi \to \Xi^0(\to \Lambda\gamma)\bar{\Xi}^0(\to \bar{\Lambda}\pi^0)$ and the dominant background $J/\psi \to \Xi^0\bar{\Xi}^0 \to \Lambda\pi^0 + \bar{\Lambda}\pi^0$ contains the nine measurable angles $\xi = (\theta_{\Xi^0}, \theta_\Lambda, \phi_\Lambda, \theta_p, \phi_p, \theta_{\bar{\Lambda}}, \phi_{\bar{\Lambda}}, \theta_{\bar{p}}, \phi_{\bar{p}})$ [40] (as illustrated in

the supplemental material [41]), where θ_{Ξ^0} is the polar angle of Ξ^0 in the J/ψ rest frame, θ_Λ ($\theta_{\bar\Lambda}$) and ϕ_Λ ($\phi_{\bar\Lambda}$) are the polar and azimuthal angles of Λ ($\bar\Lambda$) with respect to the Ξ^0 ($\bar\Xi^0$) helicity frame, and θ_p ($\theta_{\bar p}$) and ϕ_p ($\phi_{\bar p}$) are the polar and azimuthal angles of p ($\bar p$) with respect to the Λ ($\bar\Lambda$) helicity frame, respectively. With the above defined helicity angles, the differential cross section can be constructed under the helicity formalism: $d\sigma \propto \mathcal{W}(\xi)\,d\xi$, where

$$\mathcal{W} = \sum_{\mu,\bar\nu=0}^{3} \sum_{\mu'=0}^{3} \sum_{\bar\nu'=0}^{3} C_{\mu\bar\nu} a_{\mu\mu'}^{\Xi^0} a_{\mu'0}^{\Lambda} a_{\bar\nu\bar\nu'}^{\bar\Xi^0} a_{\bar\nu'0}^{\bar\Lambda}. \tag{1}$$

Here, C represents the polarization and spin correlation matrix of $\Xi^0\bar\Xi^0$, and a are the decay matrices of the hyperons (i.e. Ξ^0, $\bar\Xi^0$, Λ and $\bar\Lambda$), which depend on the decay products [41, 42]. The parameters for the matrices include α_ψ and $\Delta\Phi_\psi$ for $J/\psi \to \Xi^0\bar\Xi^0$, α_0 ($\bar\alpha_0$) and $\Delta\phi_0$ ($\Delta\bar\phi_0$) for $\Xi^0 \to \Lambda\pi^0$ ($\bar\Xi^0 \to \bar\Lambda\pi^0$), α_γ ($\bar\alpha_\gamma$) for $\Xi^0 \to \Lambda\gamma$ ($\bar\Xi^0 \to \bar\Lambda\gamma$), and α_Λ ($\bar\alpha_\Lambda$) for $\Lambda \to p\pi^-$ ($\bar\Lambda \to \bar p\pi^+$).

A Monte Carlo (MC) simulated sample of generic J/ψ decays is used to study the potential background. The signal MC samples for ST signal $e^+e^- \to J/\psi \to \Xi^0(\to$ anything$)\bar\Xi^0(\to \bar\Lambda\pi^0)$, DT signal $J/\psi \to \Xi^0(\to \Lambda\gamma)\bar\Xi^0(\to \bar\Lambda\pi^0)$ and the dominant background $J/\psi \to \Xi^0\bar\Xi^0 \to \Lambda\pi^0+\bar\Lambda\pi^0$ are generated with the amplitude according to Eq. (1). The input decay parameters for the simulation are fixed to those of the latest measurement from BESIII [32], except for α_γ and $\bar\alpha_\gamma$ which are determined in this analysis. The slight difference in reconstruction efficiencies between the signal MC samples and data is corrected with control samples [25]. Specifically, the selection efficiency for protons is studied with the control sample $J/\psi \to p\bar p\pi^+\pi^-$, the one for π^- and Λ reconstruction with the control sample $J/\psi \to \Xi^-(\to \Lambda\pi^-)\bar\Xi^+(\to \bar\Lambda\pi^+)$, the one for π^0 with the control sample $J/\psi \to \Xi^0(\to \Lambda\pi^0)\bar\Xi^0(\to \bar\Lambda\pi^0)$, and the one for photon with the control sample $J/\psi \to \gamma\mu^+\mu^-$. The correction coefficients are extracted as a function of the particle momentum and polar angle, and the efficiency corrected signal MC sample will be used to evaluate the efficiency and measure α_γ.

Charged tracks and photon candidates are detected in the main drift chamber (MDC) and electromagnetic calorimeter (EMC), and are selected individually, with the same requirements as in Ref. [32]. Particle identification (PID) is applied to select (anti-)proton candidates [32] while charged tracks other than proton candidates are regarded as pions. The $\bar\Lambda$ candidate is reconstructed with $\bar p\pi^+$ combinations, which are constrained to originate from a common vertex and are required to have an invariant mass with $\left|M_{\bar p\pi^+} - M_{\bar\Lambda}\right| < 6\,\mathrm{MeV}/c^2$, where $M_{\bar\Lambda}$ is the nominal $\bar\Lambda$ mass [36]. The π^0 candidates are reconstructed with pairs of photons whose invariant mass is within the interval $115\,\mathrm{MeV}/c^2 < M_{\gamma\gamma} < 150\,\mathrm{MeV}/c^2$, and the momenta are updated by a kine-

matic fit constraining $m_{\gamma\gamma}$ to the nominal π^0 mass [36].

The ST $\bar\Xi^0$ candidate is reconstructed with the $\bar\Lambda\pi^0$ combination whose invariant mass ($M_{\bar\Lambda\pi^0} - M_{\bar p\pi^+} + M_{\bar\Lambda}$) is closest to the nominal Ξ^0 mass (M_{Ξ^0}) from PDG [36], and is required to fall in $\left|M_{\bar\Lambda\pi^0} - M_{\bar p\pi^+} + M_{\bar\Lambda} - M_{\Xi^0}\right| < 12\,\mathrm{MeV}/c^2$. The ST yield is extracted by performing a binned maximum likelihood fit on the distribution of the recoiling mass, defined as $M_{\mathrm{rec}} = \sqrt{(E_{\mathrm{cms}} - E_{\bar p\pi^+} - E_{\pi^0})^2/c^4 - (\mathbf{p}_{\bar p\pi^+} + \mathbf{p}_{\pi^0})^2/c^2}$, where E_{cms} is the center-of-mass energy, $E_{\bar p\pi^+}$ ($\mathbf{p}_{\bar p\pi^+}$) and E_{π^0} ($\mathbf{p}_{\pi^0}$) are the energies (momenta) of $\bar\Lambda$ and π^0 in the J/ψ rest frame, respectively. The model for fitting is constructed as follows. First, a signal sample, whose π^0 is matched in the MC truth by requiring the angle between the generated and reconstructed π^0 directions less than $20°$, is obtained. Then, the signal is described with the M_{rec} distribution of this signal sample. The backgrounds of $J/\psi \to \pi^0\Lambda\bar\Sigma^0$+c.c., $J/\psi \to \Sigma^{0*}\bar\Sigma^{0*}$, and the combinatorial background of the signal are all described by the shapes of the corresponding MC simulated samples. Other backgrounds are described with a third-order polynomial function. To compensate the resolution difference between data and MC simulation, the signal shape is convolved with a Gaussian function. The fit curves are shown in the supplemental material [41]. The ST yields and the detection efficiencies evaluated with the corresponding signal MC samples are summarized in Table I.

The signal $\Xi^0 \to \Lambda\gamma$ is selected with the remaining charged and neutral tracks recoiling against the ST $\bar\Xi^0$ candidates. Events with at least one $\Lambda \to p\pi^-$ candidate and one photon are selected for further DT analysis. A five-constraint (5C) kinematic fit is performed under the hypothesis $J/\psi \to \Lambda\bar\Lambda\pi^0\gamma$, imposing overall energy-momentum conservation and requiring the π^0 candidate to have its nominal mass [36]. The χ^2 of the 5C kinematic fit ($\chi^2_{5\mathrm{C}}$) is required to be less than 40. In case of multiple candidate combinations in one event, only the one with the minimum $\chi^2_{5\mathrm{C}}$ is kept.

After the above selection, MC studies [43] indicate that the dominant sources of background events are the processes $J/\psi \to \Xi^0(\to \Lambda\pi^0)\bar\Xi^0(\to \bar\Lambda\pi^0)$ and $J/\psi \to \Sigma^0(\Sigma^{0*}) + X$, from here on referred to as BKG-I and BKG-II, respectively, where X denotes any possible particle. In particular, the decays $J/\psi \to \pi^0\Lambda\bar\Sigma^0$+c.c. and $J/\psi \to \Sigma^{0*}\bar\Sigma^{0*}$ account for a large proportion of BKG-II.

The momentum of Λ in the rest frame of Ξ^0 (p_Λ), which is well separated between the signal and BKG-I, will be used to determine the signal yield. It should be noted that $\Sigma^{0(*)}$ in BKG-II are of short lifetime, and the daughter particles of Λ and $\bar\Lambda$ originate from the same vertex point. Therefore, a powerful discrimination of signal from BKG-II requires [25] the distance L between the event primary vertex and the intersection point of Λ and $\bar\Lambda$ momentum vector to satisfy $L/\sigma_L > 2$, where σ_L is the resolution of L [44]. This requirement rejects 90 % of BKG-II events with a signal loss of less than 20 %. The

BKG-II events are further suppressed by the requirement of $\left| M_{\gamma\bar{\Lambda}} - M_{\bar{\Sigma}^0} \right| > 12\,\mathrm{MeV}/c^2$, where $M_{\gamma\bar{\Lambda}}$ is the invariant mass of γ from the signal side and $\bar{\Lambda}$ from the ST side, and $M_{\bar{\Sigma}^0}$ is the nominal $\bar{\Sigma}^0$ mass [36].
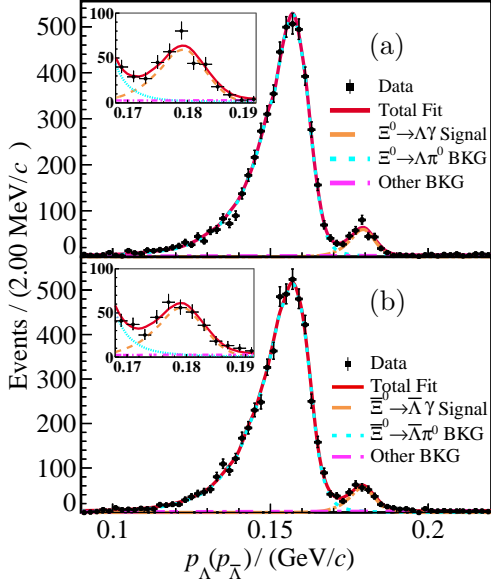

FIG. 1. Distribution of (a) p_Λ for $\Xi^0 \to \Lambda\gamma$ and (b) $p_{\bar{\Lambda}}$ for $\bar{\Xi}^0 \to \bar{\Lambda}\gamma$. The black dots with error bars are data, the red solid curves are the fit results and the orange dashed, cyan dashed and magenta dashed curves are the signal, $\Xi^0 \to \Lambda\pi^0$, and other background shapes, respectively. The inserted figures are the zoomed-in views of the signal region.

Unbinned extended maximum likelihood fits are performed on the p_Λ distributions, shown in Fig. 1, to determine the DT yields. In the fit, the shapes of the signal channel $\Xi^0 \to \Lambda\gamma$ and of the background channel $\Xi^0 \to \Lambda\pi^0$ are described with the corresponding MC simulated shapes convolved with Gaussian functions, individually, and the remaining background is described with a first-order polynomial function. The fits are performed individually for the processes $\Xi^0 \to \Lambda\gamma$ and $\bar{\Xi}^0 \to \bar{\Lambda}\gamma$, as shown in Fig. 1. A simultaneous fit between the two c.c. channels is also carried out by assuming the same BF between $\Xi^0 \to \Lambda\gamma$ and $\bar{\Xi}^0 \to \bar{\Lambda}\gamma$. As summarized in Table I, the results are well consistent with each other.

The decay asymmetry parameter is measured for the $\Xi^0 \to \Lambda\gamma$ and $\bar{\Xi}^0 \to \bar{\Lambda}\gamma$ decay channels, which after applying $0.17\,\mathrm{GeV}/c < p_\Lambda(p_{\bar{\Lambda}}) < 0.19\,\mathrm{GeV}/c$ include 371 and 391 events, respectively, with a signal purity of $\sim 77\%$. The joint likelihood function ($\mathcal{L}$) is constructed according to Eq. (1), which incorporates the set of observables ξ and a set of characterized decay parameters $H = (\alpha_\psi, \Delta\Phi_\psi, \alpha_\gamma, \bar{\alpha}_0, \Delta\bar{\phi}_0, \alpha_\Lambda, \alpha_{\bar{\Lambda}})$. The effect of the detection efficiency on $\mathcal{L}$ is evaluated by the normalization factor $\mathcal{N}$, and is calculated with the efficiency corrected signal MC sample by using the importance sampling method [45]. The target function for the

fit is $S = -\ln\mathcal{L} + \ln\mathcal{L}_{\mathrm{bkg}}$, where the contributions of background $\mathcal{L}_{\mathrm{bkg}}$ are estimated with the corresponding MC samples, including $J/\psi \to \Xi^0(\to \Lambda\pi^0)\bar{\Xi}^0(\to \bar{\Lambda}\pi^0)$, $J/\psi \to \pi^0\Lambda\bar{\Sigma}^0$+c.c. and $J/\psi \to \Sigma^{0*}\bar{\Sigma}^{0*}$ MC samples. The background likelihoods are normalized to the fitted yields of the corresponding components in the data sample. The fits are performed for the $\Xi^0 \to \Lambda\gamma$ and $\bar{\Xi}^0 \to \bar{\Lambda}\gamma$ decays individually. Furthermore, a simultaneous fit, assuming the same magnitude but opposite sign for the decay asymmetry parameters between the c.c. channels, is also performed. All fit results are shown in Table I. The effect of the decay asymmetry is visualized via three moments, each of which is calculated for $m = 8$ intervals in $\cos\theta_{\Xi^0}$:

$$M_1(\cos\theta_{\Xi^0}^k) = \frac{m}{N} \sum_{i=1}^{N_k} \sin\theta_\Lambda^i \sin\theta_{\bar{\Lambda}}^i \cos\phi_\Lambda^i \cos\phi_{\bar{\Lambda}}^i,$$

$$M_2(\cos\theta_{\Xi^0}^k) = \frac{m}{N} \sum_{i=1}^{N_k} \sin\theta_\Lambda^i \sin\phi_\Lambda^i, \qquad (2)$$

$$M_3(\cos\theta_{\Xi^0}^k) = \frac{m}{N} \sum_{i=1}^{N_k} \cos\theta_p^i,$$

where N is the total number of events, $\cos\theta_{\Xi^0}^k$ is the kth interval of $\cos\theta_{\Xi^0}$ and N_k is the number of events in the interval. Fig. 2 shows the comparison of moments between data and MC projections. The total χ^2, by averaging the χ^2 of the three moment distributions, are determined for $\Xi^0 \to \Lambda\gamma$ and $\bar{\Xi}^0 \to \bar{\Lambda}\gamma$, respectively. The total χ^2 per degree of freedom are $10.5/8$ and $10.6/8$ by comparing data to phase space MC sample, and $7.5/8$ and $7.2/8$ by comparing data to the fit results. The fit results are more consistent with data on the moment distributions.
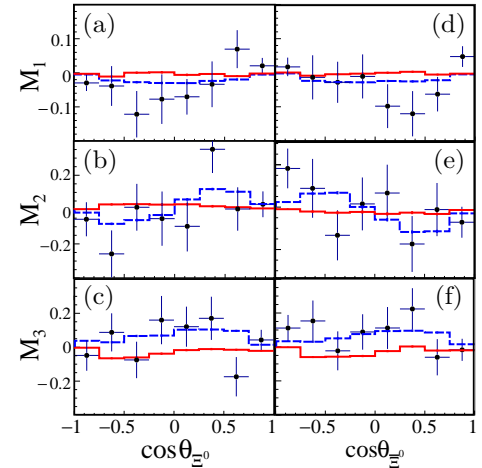

FIG. 2. Moment distributions of (a) M_1, (b) M_2 and (c) M_3 for the $\Xi^0 \to \Lambda\gamma$ decay, and (d), (e), and (f) for the $\bar{\Xi}^0 \to \bar{\Lambda}\gamma$ decay. The phase space MC events are represented by the red solid lines, the signal MC events by the blue dashed lines and the data by the black dots with error bars.

The statistical uncertainties of BFs and α_γ are determined using the error covariance matrix of the fit re-

sults [46], and the total systematic uncertainties of BFs and α_γ are studied individually. The total systematic uncertainties are summed in quadrature and are shown in Table I for the individual and c.c. combined results.

The systematic uncertainties of proton tracking and PID $(0.5\,\%)$, pion tracking $(2.3\,\%)$, Λ reconstruction $(0.9\,\%)$, and photon detection $(0.4\,\%)$ for the BF measurements are obtained as the statistical uncertainties of the efficiency correction coefficients. The uncertainties associated with the above sources for the α_γ measurement (0.001 in total) are estimated by calculating $\mathcal{N}$ from the signal MC sample without efficiency correction. The uncertainties associated with the χ^2_{5C}, L/σ_L and $m_{\gamma\bar{\Lambda}}$ requirements are estimated by applying the identical or similar requirements on the control sample of $J/\psi \to \Xi^0(\to \Lambda\pi^0)\bar{\Xi}^0(\to \bar{\Lambda}\pi^0)$, and are determined to be $0.5\,\%$ (0.001), $1.3\,\%$ (0.001), $0.2\,\%$ (0.001) for the BF (α_γ) measurement. Uncertainties from the input decay parameters [32] and α_γ are estimated by varying the input parameters within their uncertainties in the signal MC generation and in the α_γ fit, yielding the uncertainties $0.6\,\%$ for BF and 0.002 for α_γ .

The uncertainties of ST $(1.7\,\%)$ and DT $(1.8\,\%)$ yields are estimated with alternative fit scenarios, including the fit range, bin width, signal and background shapes. The uncertainties associated with the fit on α_γ are evaluated by changing the background yields within uncertainties and replacing the MC evaluated background likelihood value with that estimated with the sideband events (i.e. events satisfying $0.075 < p_\Lambda < 0.110\,\mathrm{GeV}/c$ and $0.204 < p_\Lambda < 0.216\,\mathrm{GeV}/c$), which are determined to be 0.010 and 0.012, respectively. The total uncertainties are determined to be $4.9\,\%$ $(5.2\,\%)$ for the BF of $\Xi^0 \to \Lambda\gamma$ $(\bar{\Xi}^0 \to \bar{\Lambda}\gamma)$, and $4.6\,\%$ for the c.c. combined BF result by averaging the uncorrelated uncertainties. The total uncertainties of α_γ are 0.016 (0.044) for $\Xi^0 \to \Lambda\gamma$ $(\bar{\Xi}^0 \to \bar{\Lambda}\gamma)$, and 0.019 for the combined result.

Based on the above results, two independent CP asymmetry observables are constructed,

$$\Delta_{CP} = \frac{\mathrm{BF}_+ - \mathrm{BF}_-}{\mathrm{BF}_+ + \mathrm{BF}_-} = -0.033 \pm 0.049_{\mathrm{stat.}} \pm 0.031_{\mathrm{syst.}},$$

$$A_{CP} = \frac{\alpha_\gamma + \bar{\alpha}_\gamma}{\alpha_\gamma - \bar{\alpha}_\gamma} = -0.120 \pm 0.084_{\mathrm{stat.}} \pm 0.029_{\mathrm{syst.}},$$

$$(3)$$

where BF_+ (BF_-) denotes the BF of $\Xi^0 \to \Lambda\gamma$ $(\bar{\Xi}^0 \to \bar{\Lambda}\gamma)$, and the systematic uncertainties of Δ_{CP} and A_{CP} only include the uncorrelated uncertainties. The results are consistent with zero within uncertainties.

In summary, we have performed a study of the weak radiative hyperon decay $\Xi^0 \to \Lambda\gamma$ using $\Xi^0\bar{\Xi}^0$ pairs produced in $(10\,087 \pm 44) \times 10^6$ J/ψ events collected with the BESIII detector. Benefiting from the spin entanglement between Ξ^0 and $\bar{\Xi}^0$ from J/ψ decays, the absolute BF and decay asymmetry parameter α_γ are measured with high precision. The absolute BF of this decay is

TABLE I. Individual and c.c. combined BFs and α_γ measurement results of $\Xi^0 \to \Lambda\gamma$ and $\bar{\Xi}^0 \to \bar{\Lambda}\gamma$. The first uncertainties are statistical and the second ones are systematic, if present.

Channels	$\Xi^0 \to \Lambda\gamma$	$\bar{\Xi}^0 \to \bar{\Lambda}\gamma$
$N_{\mathrm{ST}}^{\mathrm{obs}}$	$1\,400\,541 \pm 1989$	$1\,611\,216 \pm 2111$
$\varepsilon_{\mathrm{ST}}$ (%)	17.61 ± 0.01	19.77 ± 0.01
$N_{\mathrm{DT}}^{\mathrm{obs}}$	308 ± 21	330 ± 25
$\varepsilon_{\mathrm{DT}}$ (%)	4.49 ± 0.02	4.92 ± 0.02
Individual BF (10^{-3})	$1.348 \pm 0.090 \pm 0.054$	$1.326 \pm 0.098 \pm 0.066$
Combined BF (10^{-3})	$1.347 \pm 0.066 \pm 0.054$	
Individual α_γ	$-0.652 \pm 0.092 \pm 0.016$	$0.830 \pm 0.080 \pm 0.044$
Combined α_γ	$-0.741 \pm 0.062 \pm 0.019$	

$(1.347 \pm 0.066_{\mathrm{stat.}} \pm 0.054_{\mathrm{syst.}}) \times 10^{-3}$, and its decay asymmetry parameter α_γ is $-0.741 \pm 0.062_{\mathrm{stat.}} \pm 0.019_{\mathrm{syst.}}$. This work represents the first study of this decay at an electron-positron collider. The obtained results for

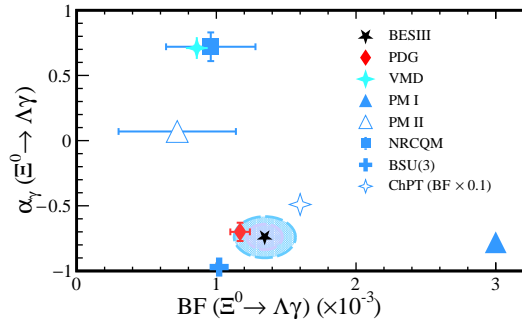FIG. 3. Distribution of α_γ versus BF of the $\Xi^0 \to \Lambda\gamma$ decay. The black star denotes the results measured by this work and the blue contours correspond to the $68\,\%/95\,\%$ confidence-level of the results. The red diamond represents the PDG values [36] of the BF and α_γ. Other symbols in blue or cyan stand for the results predicted by the vector meson dominance model (VMD) [47], pole model (PM I refers to Ref. [7] and PM II refers to Ref. [9]), nonrelativistic constituent quark model (NRCQM) [10], broken SU(3) model (BSU(3)) [48] and a ChPT theory [49]. The BF result of ChPT theory [49] is scaled down by a factor of 10 to fit within the figure.

BF and α_γ are consistent with the world average values [36] within 1.6σ and 0.6σ, respectively, but are inconsistent with various theoretical predictions. The results presented in this Letter serve as a fair confirmation of previous measurements [36] and highlight the need to improve the unified weak radiative hyperon decays theories [13, 26, 48]. This Letter also reports the first search for CP asymmetry in the decay $\Xi^0 \to \Lambda\gamma$. No evidence for CP violation is found, but its potential to study CP asymmetry in an electron-positron collider is exhibited and is expected to be further tested at the proposed Super Tau-Charm Facilities with data samples larger by two orders of magnitude [50, 51].

[1] E. Goudzovski *et al.*, Rept. Prog. Phys. **86**, 016201 (2023).

[2] I. I. Bigi, G. Ricciardi, and M. Pallavicini, *New Era for CP Asymmetries* (World Scientific, 2021).

[3] R. E. Behrends, Phys. Rev. **111**, 1691 (1958).

[4] Y. Hara, Phys. Rev. Lett. **12**, 378 (1964).

[5] M. Bazin, H. Blumenfeld, and U. Nauenberg, Phys. Rev. Lett. **14**, 154 (1965); M. Kobayashi, J. Haba, T. Homma, H. Kawai, K. Miyake, T. S. Nakamura, N. Sasao, and Y. Sugimoto, Phys. Rev. Lett. **59**, 868 (1987); S. Teige *et al.*, Phys. Rev. Lett. **63**, 2717 (1989); M. Foucher *et al.* (E761 Collaboration), Phys. Rev. Lett. **68**, 3004 (1992); T. Dubbs *et al.*, Phys. Rev. Lett. **72**, 808 (1994); A. Alavi Harati *et al.* (KTeV Collaboration), Phys. Rev. Lett. **86**, 3239 (2001).

[6] C. James *et al.*, Phys. Rev. Lett. **64**, 843 (1990).

[7] M. B. Gavela, A. L. Yaouanc, L. Oliver, O. Pène, J. C. Raynal, and T. N. Pham, Phys. Lett. B **101**, 417 (1981).

[8] Y. I. Kogan and M. A. Shifman, Sov. J. Nucl. Phys. **38**, 628 (1983).

[9] G. Nardulli, Phys. Lett. B **190**, 187 (1987).

[10] P. Y. Niu, J. M. Richard, Q. Wang, and Q. Zhao, Chin. Phys. C **45**, 013101 (2020).

[11] I. I. Balitsky, V. M. Braun, and A. V. Kolesnichenko, Nucl. Phys. B **312**, 509 (1989); D. Chang, arXiv:hep-ph/0011163 (2000); E. N. Dubovik, V. S. Zamiralov, S. N. Lepshokov, and A. E. Shkolnikov, Phys. At. Nucl. **71**, 136 (2008); P. Zenczykowski, Acta Phys. Polon. B **51**, 2111 (2020).

[12] R. C. Verma and A. Sharma, J. Phys. G **12**, 1329 (1986).

[13] R. X. Shi, S. Y. Li, J. X. Lu, and L. S. Geng, Sci. Bull. **67**, 2298 (2022).

[14] R. X. Shi and L. S. Geng, Sci. Bull. **68**, 779 (2023).

[15] A. D. Sakharov, Pisma Zh. Eksp. Teor. Fiz. **5**, 32 (1967).

[16] J. H. Christenson, J. W. Cronin, V. L. Fitch, and R. Turlay, Phys. Rev. Lett. **13**, 138 (1964); B. Aubert *et al.* (BaBar Collaboration), Phys. Rev. Lett. **87**, 091801 (2001); K. Abe *et al.* (Belle Collaboration), Phys. Rev. Lett. **87**, 091802 (2001); R. Aaij *et al.* (LHCb Collaboration), Phys. Rev. Lett. **122**, 211803 (2019).

[17] G. Costa and P. K. Kabir, Phys. Rev. Lett. **18**, 429 (1967); G. Ecker, A. Pich, and E. de Rafael, Nucl. Phys. B **303**, 665 (1988); H. Y. Cheng, Phys. Lett. B **315**, 170 (1993); Phys. Rev. D **49**, 3771 (1994).

[18] N. Adolph, J. Brod, and G. Hiller, Eur. Phys. J. C **81**, 45 (2021); S. de Boer and G. Hiller, JHEP **08**, 091 (2017).

[19] D. Atwood, M. Gronau, and A. Soni, Phys. Rev. Lett. **79**, 185 (1997); J. M. Soares, Nucl. Phys. B **367**, 575 (1991); M. Beneke, T. Feldmann, and D. Seidel, Eur. Phys. J. C **41**, 173 (2005); M. Matsumori, A. I. Sanda, and Y. Y. Keum, Phys. Rev. D **72**, 014013 (2005); P. Ball, G. W. Jones, and R. Zwicky, Phys. Rev. D **75**, 054004 (2007).

[20] C. Delaunay, J. F. Kamenik, G. Perez, and L. Randall, JHEP **01**, 027 (2013); J. Lyon and R. Zwicky, Phys. Rev. D **106**, 053001 (2022); A. Paul and D. M. Straub, JHEP **04**, 027 (2017); A. Biswas, S. Mandal, and N. Sinha, Int. J. Mod. Phys. A **33**, 1850194 (2018).

[21] G. Isidori and J. F. Kamenik, Phys. Rev. Lett. **109**, 171801 (2012); G. Bhattacharyya, D. Chang, C. H. Chou, and W. Y. Keung, Phys. Lett. B **493**, 113 (2000).

[22] X. L. Chen, C. S. Gao, and X. Q. Li, Phys. Rev. D **51**, 2271 (1995); S. S. Nair, E. Perotti, and S. Leupold, Phys. Lett. B **788**, 535 (2019); G. Hiller and A. Kagan, Phys. Rev. D **65**, 074038 (2002); N. Adolph and G. Hiller, Phys. Rev. D **105**, 116001 (2022).

[23] E. J. Ramberg *et al.* (E731 Collaboration), Phys. Rev. Lett. **70**, 2529 (1993); J. P. Lees *et al.* (BaBar Collaboration), Phys. Rev. Lett. **109**, 191801 (2012); T. Saito *et al.* (Belle Collaboration), Phys. Rev. D **91**, 052004 (2015); A. Abdesselam *et al.* (Belle Collaboration), Phys. Rev. Lett. **118**, 051801 (2017); T. Horiguchi *et al.* (Belle Collaboration), Phys. Rev. Lett. **119**, 191802 (2017).

[24] R. Aaij *et al.* (LHCb Collaboration), Phys. Rev. D **105**, L051104 (2022).

[25] M. Ablikim *et al.* (BESIII Collaboration), Phys. Rev. Lett. **130**, 211901 (2023).

[26] J. Lach and P. Zenczykowski, Int. J. Mod. Phys. A **10**, 3817 (1995).

[27] V. Fanti *et al.* (NA48 Collaboration), Eur. Phys. J. C **12**, 69 (2000).

[28] A. Lai *et al.* (NA48 Collaboration), Phys. Lett. B **584**,

251 (2004).

[29] J. R. Batley *et al.*, Phys. Lett. B **693**, 241 (2010).

[30] M. Ablikim *et al.* (BESIII Collaboration), Nature Phys. **15**, 631 (2019); Phys. Rev. Lett. **126**, 092002 (2021); Phys. Rev. Lett. **125**, 052004 (2020); JHEP **11**, 226 (2021); Nature **606**, 64 (2022); M. Ablikim *et al.* (BESIII), (2024), arXiv:2406.06118 [hep-ex].

[31] M. Ablikim *et al.* (BESIII Collaboration), arXiv:2309.14667 [hep-ex].

[32] M. Ablikim *et al.* (BESIII Collaboration), Phys. Rev. D **108**, L031106 (2023).

[33] P. C. Hong, R. G. Ping, T. Luo, X. R. Zhou, and H. Li, Chin. Phys. C **47**, 093103 (2023).

[34] R. M. Baltrusaitis *et al.* (MARK III Collaboration), Phys. Rev. Lett. **56**, 2140 (1986).

[35] M. Ablikim *et al.* (BESIII Collaboration), Phys. Rev. Lett. **129**, 212002 (2022).

[36] R. L. Workman *et al.* (Particle Data Group), PTEP **2022**, 083C01 (2022).

[37] M. Ablikim *et al.* (BESIII Collaboration), Chin. Phys. C **46**, 074001 (2022).

[38] M. Ablikim *et al.* (BESIII Collaboration), Nucl. Instrum. Meth. A **614**, 345 (2010).

[39] W. Li *et al.*, Proc. Int. Conf. Comput. High Energy and Nucl. Phys , 225 (2006); D. M. Asner *et al.*, Int. J. Mod. Phys. A **24S1**, 499 (2009); J. Zhang *et al.*, Radiat. Detect. Technol. Methods **2**, 1 (2018).

[40] E. Perotti, G. Fäldt, A. Kupsc, S. Leupold, and J. J. Song, Phys. Rev. D **99**, 056008 (2019).

[41] See Supplemental Material at `URL to be inserted by publisher` for additional details.

[42] V. Batozskaya, A. Kupsc, N. Salone, and J. Wiechnik, Phys. Rev. D **108**, 016011 (2023).

[43] X. Zhou, S. Du, G. Li, and C. Shen, Comput. Phys. Commun. **258**, 107540 (2021).

[44] M. Xu *et al.*, Chin. Phys. C **34**, 92 (2010).

[45] T. Kloek and H. K. van Dijk, Econometrica **46**, 1 (1978).

[46] F. James and M. Roos, Comput. Phys. Commun. **10**, 343 (1975).

[47] P. Zenczykowski, Phys. Rev. D **44**, 1485 (1991).

[48] P. Zenczykowski, Phys. Rev. D **73**, 076005 (2006).

[49] B. Borasoy and B. R. Holstein, Phys. Rev. D **59**, 054019 (1999).

[50] A. E. Bondar *et al.* (Charm-Tau Factory Collaboration), Phys. Atom. Nucl. **76**, 1072 (2013).

[51] M. Achasov *et al.*, Front. Phys. **19**, 14701 (2024).